



Cite this: *Mater. Chem. Front.*,  
2023, 7, 5466

Received 1st August 2023,  
Accepted 12th September 2023

DOI: 10.1039/d3qm00853c

[rsc.li/frontiers-materials](http://rsc.li/frontiers-materials)

# High-performance perovskite light-emitting diodes based on grain boundary passivation: progress, challenges and perspectives

Yalian Weng, Eng Liang Lim,  Yuanyuan Meng, Junpeng Lin and Zhanhua Wei \*

Metal halide perovskites are emerging as promising candidates for next-generation display and lighting technologies. In less than 10 years, the external quantum efficiency (EQE) of perovskite light-emitting diodes (PeLEDs) has skyrocketed from 0.1% to around 30%. Herein, we briefly introduce PeLEDs and summarise our group's progress in preparing PeLEDs using the strategy of grain boundary passivation. Then, we present the challenges and future outlooks toward the further development of PeLEDs. We hope that this perspective can bring informative guidance and innovative ideas to the PeLED community.

## 1. Introduction

Metal halide perovskites with the chemical structure of  $ABX_3$  have attracted attention owing to their excellent optoelectrical properties, such as tunable emission wavelength, narrow full width at half-maximum (FWHM), long carrier diffusion length, high color purity and wide color gamut.<sup>1–5</sup> Generally, A is a monovalent organic or inorganic cation, B is a divalent metallic cation, and X is a halide anion (e.g., A:  $\text{Cs}^+$ ,  $\text{CH}_3\text{NH}_3^+$  ( $\text{MA}^+$ ),  $\text{CH}(\text{NH}_2)_2^+$  ( $\text{FA}^+$ ); B:  $\text{Pb}^{2+}$ ,  $\text{Sn}^{2+}$ ; X:  $\text{Cl}^-$ ,  $\text{Br}^-$ ,  $\text{I}^-$ ).<sup>2,6,7</sup> Since the first report of solution-processed PeLEDs that operated at room temperature in 2014,<sup>8</sup> various types of strategies, *i.e.*, additive engineering, interface engineering, composition engineering and so on, have been carried out to improve the performance and stability of PeLEDs. In just a decade of development, the maximum EQEs of the green, red and near-infrared-based PeLEDs have exceeded 20%.<sup>9–13</sup> In this perspective, we introduce the working principle of PeLEDs and summarize our recent efforts in developing highly efficient PeLEDs with the  $\text{EQE} > 20\%$  through perovskite grain boundary passivation. At the same time, a detailed discussion of the challenges and the future outlooks toward the development of PeLEDs is also presented.

## 2. Basic working principle of PeLEDs

PeLEDs can be categorized into p-i-n and n-i-p structures depending on the deposition sequence of the carrier transport

*Xiamen Key Laboratory of Optoelectronic Materials and Advanced Manufacturing, Institute of Luminescent Materials and Information Displays, College of Materials Science and Engineering, Huaqiao University, Xiamen 361021, China.*  
E-mail: [weizhanhua@hqu.edu.cn](mailto:weizhanhua@hqu.edu.cn)

layer (CTL) (Fig. 1(a) and (b)). When a forward voltage is applied to the device, the holes from the anode and the electrons from the cathode are injected into a hole transport layer (HTL) and an electron transport layer (ETL), respectively. Under an applied electric field, these charge carriers are drifted to a perovskite emitter layer and recombine radiatively, producing electroluminescence (Fig. 1(c)). The emission color or wavelength produced by PeLEDs depends on the energy bandgap ( $E_g$ ) of the perovskite materials. For example, perovskite materials with iodide-dominant and chloride-dominant compositions can produce infrared and blue light, respectively. To minimize the exciton quenching and non-radiative recombination of the PeLEDs, it is essential to optimize (i) the quality of the perovskite film, (ii) the charge injection into PeLEDs, (iii) the energy level alignment, (iv) the interface contact, and (v) the physical and chemical properties of each functional layer. Through electrical and optical characterization studies, the performance of PeLEDs, such as EQE, luminance and current efficiency, can be obtained.

## 3. Grain boundary passivation strategies

Nowadays, a spin-coating method has been widely used to prepare the perovskite films for optoelectronic applications. However, the perovskite films derived from the solution-processing methods usually exhibit poor surface coverage with a large number of bulk/surface defects attributed to the uncontrollable perovskite crystallization rate during the film formation process.<sup>14–17</sup> To optimize the perovskite film quality with the enhanced electrical and chemical properties of PeLED applications, we have developed a series of grain boundary passivation strategies: halide passivation, non-halide passivation

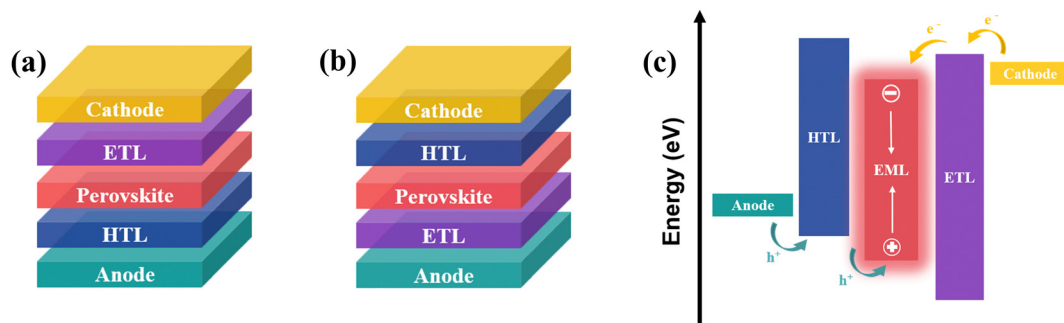


Fig. 1 Typical structures of the PeLED device: (a) p-i-n structure and (b) n-i-p structure. (c) Schematic diagram of the electroluminescence mechanism of PeLEDs.

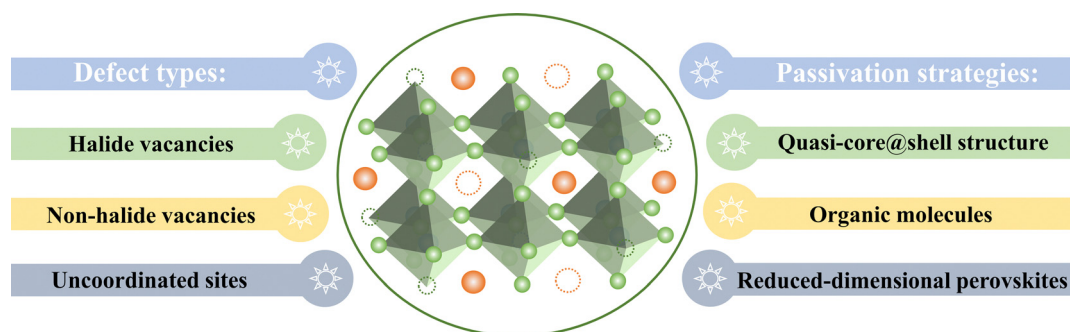


Fig. 2 Defect classification of perovskite films and the corresponding grain boundary passivation strategies.

and their combination (Fig. 2). In the following subsections, we will introduce these strategies in detail for fabricating highly efficient and stable PeLEDs.

### 3.1. Halide passivation

It is well-known that the number of defects/vacancies induced on the perovskite film surface/bulk film highly depends on the perovskite crystallization rate process. And it is hard to obtain a high-quality  $\text{CsPbBr}_3$  emitter layer due to its fast and uncontrollable crystallization.<sup>18–20</sup> To overcome this problem, our group introduced the methylammonium bromide (MABr) additive to the  $\text{CsPbBr}_3$  perovskite precursor to modulate the corresponding crystallization process (Fig. 3(a)). Because of the very different solubility between  $\text{CsPbBr}_3$  and MABr in DMSO ( $\text{CsPbBr}_3$ :  $\sim 0.56$  M, MABr:  $> 5$  M), MABr could sequentially crystallize after the  $\text{CsPbBr}_3$  precursor was wholly consumed, yielding the  $\text{CsPbBr}_3$ @MABr quasi-core@shell structure.<sup>9</sup> In this study, we found that the addition of MABr not only passivated the perovskite surface and grain boundaries but also facilitated the balance charge injection into the PeLEDs. Benefitting from these, the non-radiative recombination of PeLEDs was suppressed, yielding higher photoluminescence efficiency with a longer device lifetime. To further improve the charge injection balance of PeLEDs, poly(methyl methacrylate) (PMMA) was spin-coated at the perovskite/B3PYMPM interface (Fig. 3(b)). A maximum EQE of 20.31% (Fig. 3(c)) with a  $T_{50}$  of more than 100 h (Fig. 3(d)) was achieved for the dual-

modification device, which was the best-reported performing PeLED in 2018.

Encouraged by the performance enhancement from MABr, we concluded that halide salt could modulate the crystallization process and affect the as-formed film's morphology, composition and spatial distribution. However, MABr is an organic salt and may suffer from ion migration and decomposition issues when the PeLEDs are driven at a high voltage. Hence, we tried to use the more thermally stable formamidinium bromide (FABr). Interestingly, adding FABr to the perovskite precursor not only induced the quasi-core@shell structure formation but also initiated a chemical reaction and formed the  $\text{Cs}_4\text{PbBr}_6$  interlayer. Benefited from the formation of  $\text{CsPbBr}_3$ @ $\text{Cs}_4\text{PbBr}_6$ @MABr&FABr quasi-core@shell structure, the vacancy defects (*i.e.*,  $\text{Cs}^+$  and  $\text{Br}^-$ ) and the non-radiative recombination center (*i.e.*, uncoordinated Pb atom) of the  $\text{CsPbBr}_3$  perovskite were significantly suppressed.<sup>21</sup> Additionally,  $\text{Cs}_4\text{PbBr}_6$  with a suitable thickness can form a type-I heterojunction with  $\text{CsPbBr}_3$  to confine charge carriers in the  $\text{CsPbBr}_3$  crystals, increasing the radiative recombination efficiency (Fig. 4(a)). Therefore, the phase ratio of  $\text{Cs}_4\text{PbBr}_6$  on  $\text{CsPbBr}_3$  was optimized to enhance the performance of perovskite films and devices (Fig. 4(b)). When the molar ratio of  $\text{CsPbBr}_3$ :MABr:FABr was 1:0.8:0.2, the PeLEDs (Fig. 4(d)) exhibited superior device performance (*i.e.*, a maximum EQE of 22.3% and a higher luminance of  $10\,050$   $\text{cd m}^{-2}$ ) with a longer device lifetime (*i.e.*,  $T_{50}$  of 59 h at  $130$   $\text{cd m}^{-2}$ ) (Fig. 4(c), (e), and (f)).

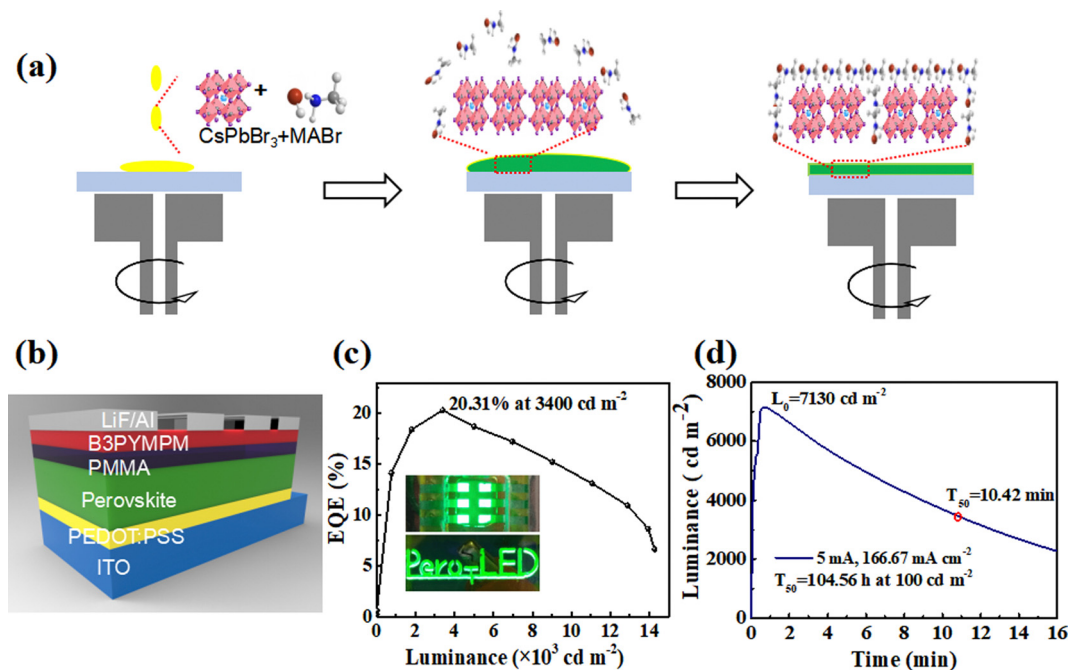


Fig. 3 (a) Formation process diagram of the CsPbBr<sub>3</sub>@MABr quasi-core@shell structure. (b) Structure of the PeLED device. (c) EQE–L characteristic and (d) lifetime measurement of the best-performing PeLEDs. Reproduced with permission from ref. 9. Copyright 2018, Springer Nature Limited.

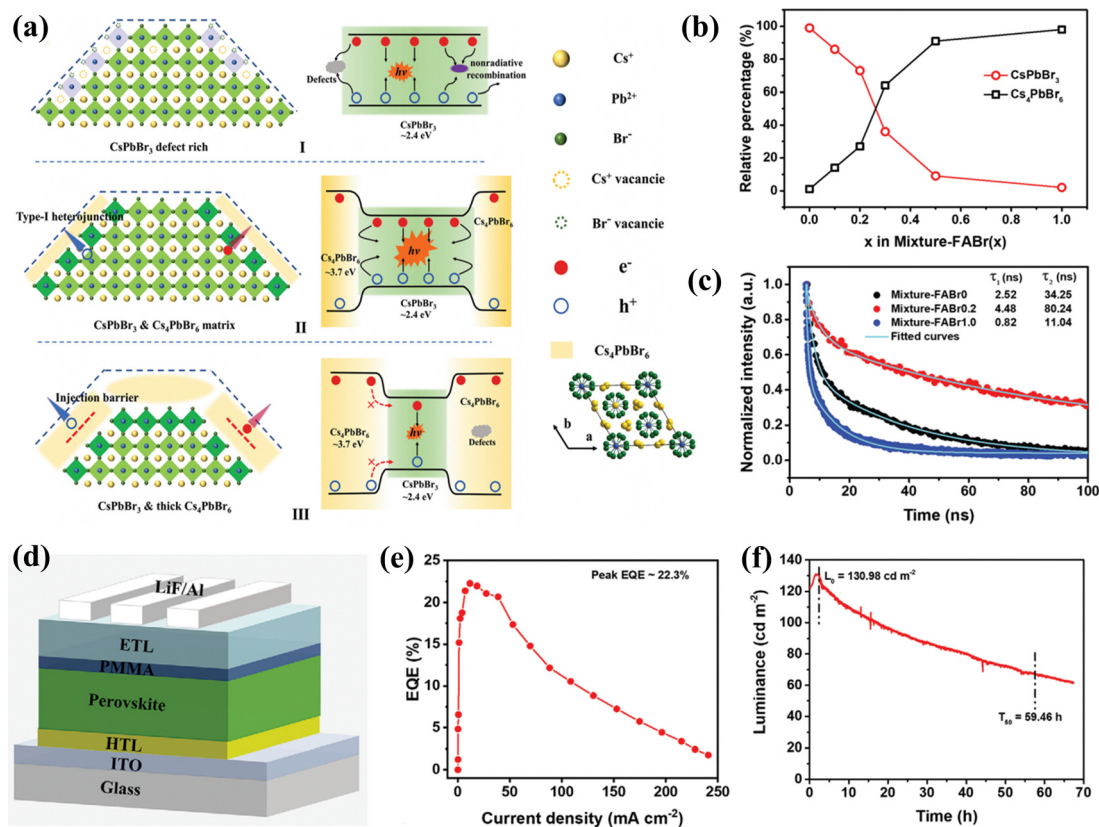


Fig. 4 (a) Schematic illustration of the three typical phase compositions and their impact on defect passivation. (b) The relative percentages of CsPbBr<sub>3</sub> and Cs<sub>4</sub>PbBr<sub>6</sub> in various mixture perovskite films. (c) PL-decay curves of the three typical perovskite films. (d) Structure of the PeLED device. (e) EQE–J characteristics and (f) lifetime measurements of the best-performing PeLEDs. Reproduced with permission from ref. 21. Copyright 2022, Wiley-VCH GmbH.

### 3.2 Non-halide passivation

In addition to halide-based materials, organic molecules, such as Lewis bases, Lewis acids, and alkylammonium salt, have also been widely used to passivate the ion defects and balance the charge injection of the perovskite emission layer.<sup>22–25</sup> Currently, trioctylphosphine oxide (TOPO) and triphenylphosphine oxide (TPPO) are the commonly used non-halide passivator in PeLEDs. However, these organic molecules are insulators and not beneficial for the charge injection/charge transport in the devices.<sup>26,27</sup> Aiming to solve this problem, our group proposed a bifunctional conductive molecule with two phosphine oxide functional groups, namely 2,7-bis(diphenylphosphoryl)-9,9'-spirobifluorene (SPPO13) as a passivation layer for CsPbBr<sub>3</sub>-based PeLED applications (Fig. 5(a)).<sup>28</sup> With the addition of SPPO13, the P=O functional groups of SPPO13 could donate its lone electron pair on the oxygen atom to the empty 6p orbital of Pb<sup>2+</sup> of the perovskite, thus, leading to the chemical changes of Pb<sup>2+</sup> and Br<sup>-</sup> and the decrease of defect density. As a result, the surface defects of the perovskite were passivated, and the electron injection at the perovskite/ETL interface was promoted. Finally, the modified PeLEDs presented a maximum EQE of 22.3% with a maximum brightness of around 190 000 cd m<sup>-2</sup> (Fig. 5(b) and (c)).

Meanwhile, it has also been reported that polymers with different functional groups can interact with the perovskite grains to passivate the perovskite surface/bulk defects.<sup>29</sup> For example, poly(vinylidene fluoride) (PVDF) with abundant F atoms was able to passivate both the organic cation and halide anion vacancies by forming hydrogen bonds (N–H···F) with organic cations (MA/FA) and ionic bonds with Pb<sup>2+</sup> in the perovskite films, boosting the performance of PeLEDs.<sup>30</sup> In contrast to the traditional surface treatment (Fig. 6(a)), our group recently showed that the infiltrative treatment method (Fig. 6(b)) enabled PVDF in the perovskite matrix to distribute on the perovskite

grain boundary and the surface more evenly, increasing the PL intensity and lifetime of perovskite films (Fig. 6(c) and (d)). During the film formation process, the PVDF polymer could regulate the perovskite crystal growth and passivate the perovskite surface/bulk defects. Meanwhile, the film derived from the infiltrative treatment method exhibited a more compact film surface with tightly packed crystals. As a result, the non-radiative recombination and the energy loss were significantly suppressed. Finally, a maximum EQE of 22.29% with excellent reproducibility was achieved (Fig. 6(e), (f) and (g)).

### 3.3 Combination of passivation strategies

3D perovskites can be transformed to quasi-2D perovskites (*i.e.*, reduced dimensional perovskites (RDPs)) by adding large organic molecules into the A-site of 3D perovskites. Generally, RDPs consisting of quantum wells (QWs) separated by organic intercalating cations possess high exciton binding energies, which can increase the stability and the photoluminescence quantum yield (PLQY) of PeLEDs. However, the uneven QW thickness will induce energy disorders. Thus, RDP films show several problems of chaotic *n* value, different dimensions, non-radiative recombination defects and carrier transport difficulties, resulting in poor EQE with inferior color purity for RDP-based LEDs.

To manipulate the crystallization rate of RDPs, we synthesized a bifunctional molecule containing fluorine atoms and a phosphine oxide (P=O) functional group, namely tris(4-fluorophenyl) phosphine oxide (TFPPO). The TFPPO was dissolved in chloroform and then used as an antisolvent to modify the preparation of the PEA<sub>2</sub>Cs<sub>1.6</sub>MA<sub>0.4</sub>Pb<sub>3</sub>Br<sub>10</sub> film.<sup>31</sup> With TFPPO, the strong electronegativity of the F atom could form hydrogen bonds with the organic cations in the perovskite to serve as a diffusion controller during the RDP film formation process (Fig. 7(a)). On the other hand, phosphine oxide (P=O) of TFPPO could bind to the unsaturated sites at the perovskite

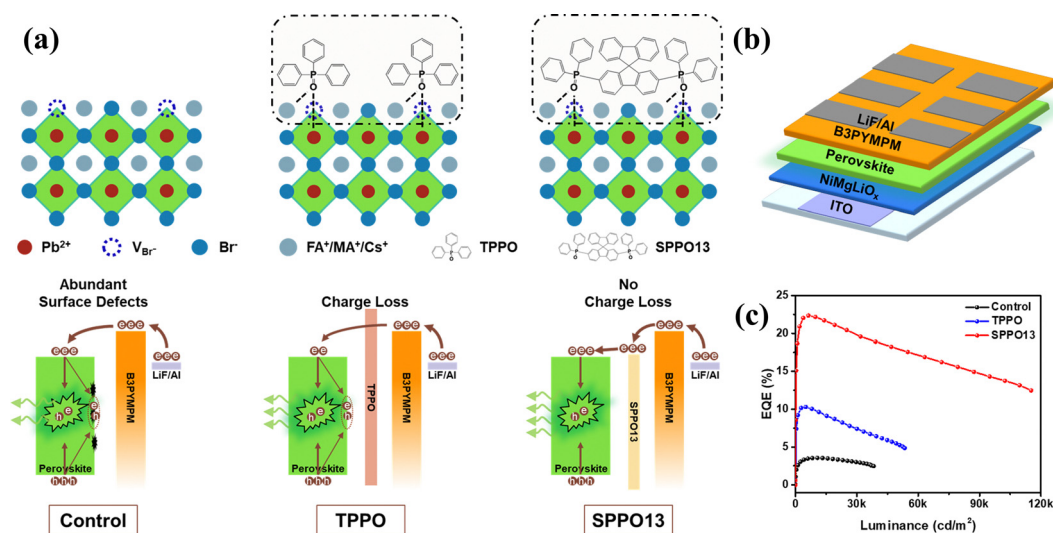


Fig. 5 (a) Schematic illustration of the control, TPPO- and SPPO13-treated samples and the corresponding charge injection and recombination process. (b) Structure of the PeLED device. (c) EQE-L characteristics of the control, TPPO-treated and SPPO13-treated PeLEDs. Reprinted (adapted) with permission from ref. 28. Copyright 2022, American Chemical Society.

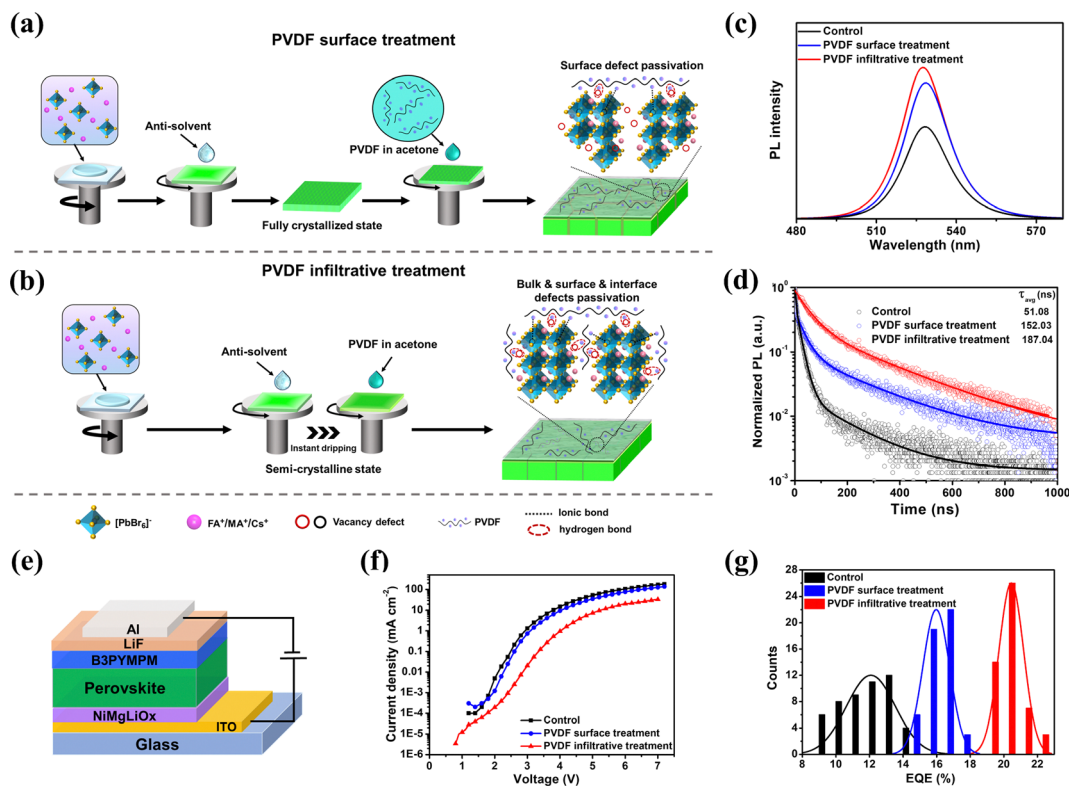


Fig. 6 Schematic diagrams of treating perovskite films with PVDF via (a) surface treatment and (b) infiltrative treatment. The measurement of (c) steady PL spectra and (d) TRPL decay curves of the control, surface treatment, and infiltrative treatment films, respectively. (e) Structure of the PeLED device. (f)  $J$ - $V$  characteristics and (g) EQE statistics histogram of the control, surface treatment, and infiltrative treatment PeLEDs. Reproduced with permission from ref. 30. Copyright 2022, Wiley-VCH GmbH.

grain boundaries to reduce the defect density of the perovskite film. Benefitting from these, an enhanced PLQY with excellent device performance (*i.e.*, a maximum EQE of 25.6%) was obtained for the modified PeLEDs (Fig. 7(b)), as well as a longer device lifetime (Fig. 7(c), (d) and (e)). This work highlights that the combination of macromolecular halogen ammonium salt (halide passivation) and organic passivation molecules (non-halide passivation) could provide a new pathway to improve the performance of PeLEDs.

## 4. Challenges and perspectives of PeLEDs

Halide perovskites are excellent materials for research on perovskite solar cells (PSCs) and PeLEDs. Even though a high performance of 30.84% has been achieved for lead-based PeLEDs (Pb-PeLEDs),<sup>32</sup> the toxicity of the lead (Pb) element in perovskites still remains a big challenge and can further hinder the development of PeLEDs. Meanwhile, the perovskite-based emission and functional layers also show poor ambient, thermal and light stability.<sup>33–38</sup> To our knowledge, the operational stability of PeLEDs nowadays is excellently low compared to the inorganic LEDs, mostly due to the dissociation and ion migration of the perovskite material itself.<sup>33,39–41</sup> To facilitate

the commercialization of PeLEDs, the as-mentioned above issues need to be resolved.

Because the Pb element in perovskites is harmful to humans and the environment, developing Pb-free PeLEDs is greatly important for PeLED applications. In general,  $\text{Pb}^{2+}$  can be replaced by  $\text{Sn}^{2+}$ ,  $\text{Sb}^{2+}$ ,  $\text{Mn}^{2+}$ ,  $\text{Cu}^{2+}$  and other elements.<sup>42</sup> Among them,  $\text{Sn}^{2+}$  is considered as one of the potential candidates, which belongs to the same group element as Pb and has similar physical and chemical properties to those of  $\text{Pb}^{2+}$ . Compared with  $\text{Pb}^{2+}$ ,  $\text{Sn}^{2+}$  possess a lower energy band gap and higher charge mobility. More importantly,  $\text{SnO}_2$ , which degrades from Sn-based perovskites exposed to ambient air, is an environmentally friendly material that does not pollute the environment. Thus, we believe that the Sn-based perovskite emission layer will become a spot research material in PeLED applications. Recently, our group has achieved an impressive EQE of 5.4% based on the Sn-perovskite emitter (*i.e.*, the highest recorded efficiency to date for  $\text{CsSnI}_3$  PeLEDs).<sup>43</sup> However, the EQE of Sn-PeLEDs is much lower when compared with Pb-PeLEDs, attributed to the poor film morphology and the imbalance carrier transport of the Sn-based perovskite material, which needs to be further promoted. For the efficiency enhancement and stability improvement of PeLEDs, several promising strategies of device engineering (*i.e.*, additive engineering, interface engineering, perovskite dimensionality manipulation and so on) are proposed as follows:

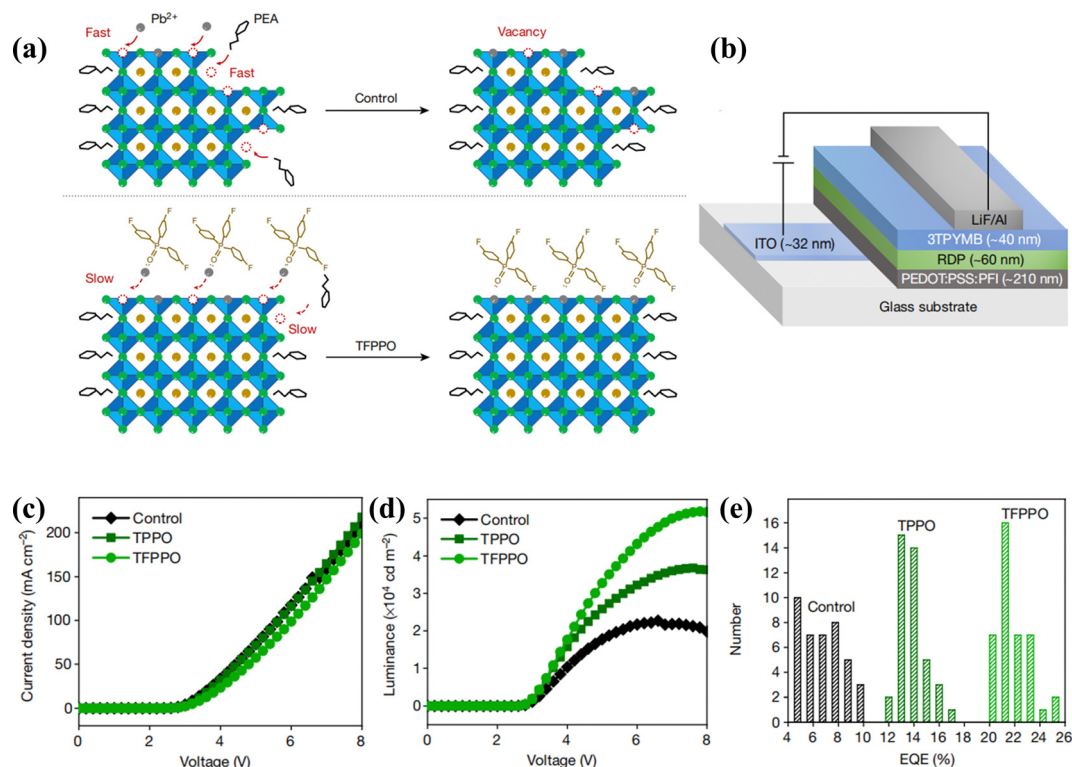


Fig. 7 (a) Schematic illustration of the preparation of perovskite films with and without TFPPO. (b) Structure of the PeLED device. (c)  $J$ - $V$  characteristics, (d)  $L$ - $V$  characteristics and (e) EQE histogram of the control, TPPO-treated, and TFPPO-treated PeLEDs. Reproduced with permission from ref. 31. Copyright 2021, Springer Nature Limited.

(I) Dimensionality manipulation: Typically, the non-radiative recombination rate is higher than the radiative recombination rate for three-dimensional (3D) perovskites, attributed to its lower exciton binding energy and longer carrier diffusion length. In contrast, the RDP exhibits excellent electrical properties, which is beneficial to facilitate the charge carrier injection into the perovskite emission layer.<sup>44,45</sup> For example, it has been demonstrated that the natural quantum well 2D perovskite can limit the charge carrier within a specific region inside the emission layer. Due to the quantum restriction and dielectric confinement effect, the 2D perovskite exhibits higher exciton binding energy with excellent luminescence properties.<sup>44</sup> Compared with 3D perovskites, 2D perovskites exhibit higher operational stability under light, thermal and ambient stress conditions. As such, it can be seen that manipulation of perovskite dimensionality is one of the effective methods to improve the performance and stability of PeLEDs.

(II) Additive engineering: It is generally accepted that slow nucleation and fast crystallization rates of the perovskite during the film formation process can induce a poor film morphology (*i.e.*, many defective states) with lower fluorescence quantum efficiency. To regulate the crystallization rate and minimize the bulk/surface defect of perovskites, the addition of additives such as slow release agents and/or passivating agents (*i.e.*, small organic molecules, polymers and metallic salts and so on) in the perovskite precursor solution and antisolvent solution during the film deposition process is proposed to control the precipitation of perovskite grains step by step or time by time (Fig. 8(a)),

which is an effective way to boost the quality and photoelectric properties of perovskite films.

(III) Device structure modification: Each functional layer of PeLEDs has a crucial impact on the device performance and stability. Thus, it is important to carefully optimize the functional layer to optimize the charge carrier injection into the perovskite emission layer. For example, the conduction/valence band of ETL/HTL must well match with the lowest unoccupied molecular orbital (LUMO)/the highest occupied molecular orbital (HOMO) of perovskites so that the electrons/holes can be injected into the perovskite emitting layer effectively at a higher radiative recombination rate (Fig. 8(b)). In addition, modification at HTL/perovskite and perovskite/ETL interfaces can further reduce the trap states and the charge accumulation of PeLEDs. Taking advantages of these, lower non-radiative recombination loss with higher EQE of PeLEDs can be realized.

(IV) Light extraction efficiency optimization: It is well-known that the EQE of PeLEDs is determined by the internal quantum efficiency (IQE) and the light extraction efficiency (LEE), where the IQE can be increased to nearly 100% by optimizing the materials and device structures. However, the poor LEE of PeLEDs usually restricts the EQE of PeLEDs at <30%,<sup>13,46-48</sup> attributed to the optical interaction between the various surfaces. A large number of photons are trapped or lost due to the total reflection and waveguide mode at the interface between air, functional layers and substrate, and the surface plasmon-polariton (SPP) mode at the metal cathode surface, unable to escape the device. Therefore, minimizing the total

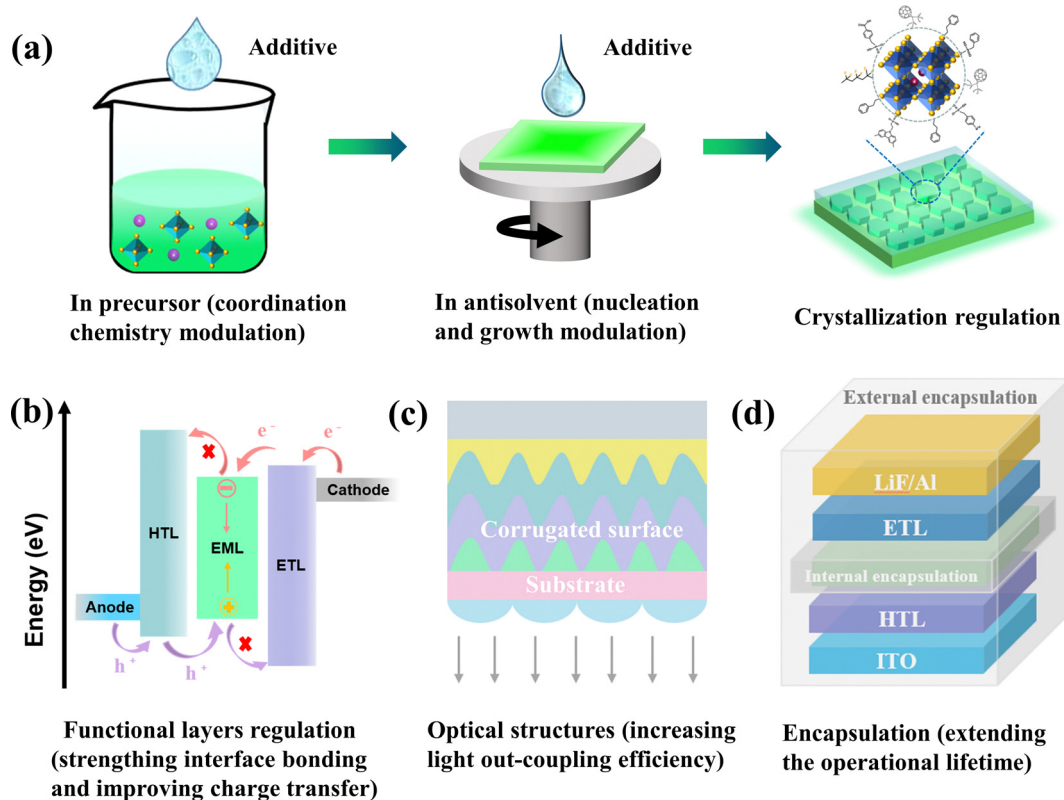


**Fig. 8** Strategy diagrams for improving the efficiency and stability of PeLEDs. (a) Additive engineering: introduce additives in the precursor or the antisolvent to regulate the crystallization process of perovskites. (b) Device structure: select suitable functional layers to improve radiative recombination. (c) Light extraction efficiency: adopt the corrugated surface or optical micro–nano structures to enhance the light out-coupling efficiency. (d) Internal and external encapsulations: encapsulate perovskite crystals or PeLED devices to increase the lifetime and stability.

reflection, waveguide, and SPP modes of PeLEDs is important to increase the device's LEE performance. Various strategies are proposed to increase the light out-coupling efficiency, such as employing the wrinkle structure, nano-scattering layer, microlens arrays, optical structure and corrugated surface in PeLEDs (Fig. 8(c)). Improving the LEE will be the key to boosting EQE to over 30%.

(V) External and internal encapsulation: Perovskite materials are susceptible to water vapor and oxygen, leading to poor environmental stability. Therefore, it is crucial to encapsulate the PeLED device to protect them from external erosion. According to the location of the protective layer, encapsulation can be divided into internal encapsulation and external encapsulation, which are inside and outside the device, respectively (Fig. 8(d)). The internal encapsulation can be divided into upper and lower encapsulations according to its position relative to the perovskite material, which is essential for passivating surface defects, inhibiting ion migration, balancing charge injection and improving the stability of the perovskite emitting layer. By contrast, the external encapsulation can be divided into glass plate and thin film encapsulations, which are available for the flexible device. And the thin film encapsulation layer can be an inorganic layer, organic layer, or alternating inorganic–organic layer. Among them, the inorganic thin films (*i.e.*,  $\text{Al}_2\text{O}_3$ ,  $\text{TiO}_2$ ,  $\text{ZrO}_2$ ,  $\text{Si}_3\text{N}_4$  and so on) serve as the main moisture/oxygen barrier, while the organic thin films (*i.e.*, PMMA, PDMS, NOA and so on) are mainly responsible for filling

the holes in the inorganic layer and prolonging the diffusion pathways for water vapor and oxygen. Generally, the inorganic layers can be obtained by atomic layer deposition (ALD), magnetron sputtering and thermal evaporation, while the organic layers can be prepared by spin coating, ink-jet printing, screen printing and other methods.

## 5. Conclusions

In conclusion, we have summarized our recent advances in high-performance PeLEDs using the grain boundary passivation strategy. Meanwhile, we also provide the challenges and future outlooks of PeLEDs. Even though highly efficient PeLEDs with an EQE of 30.84% have been realized, further efforts (*i.e.*, perovskite dimension regulation, additive engineering, device structure design, encapsulation and light extraction efficiency improvement) are still required to further enhance the performance and stability of PeLEDs. Our group firmly believes that PeLEDs will serve as a promising technology for the next-generation displays and lighting in the future.

## Conflicts of interest

There are no conflicts to declare.

## Acknowledgements

This work was financially supported by the National Natural Science Foundation of China (62204089 and U21A2078), Natural Science Foundation of Fujian Province (2020J06021 and 2020J01064), the Promotion Program for Young and Middle-aged Teacher in Science and Technology Research of Huaqiao University (ZQN-1124) and the Scientific Research Funds of Huaqiao University (21BS132).

## References

- J. Zhang, P. P. Shum and L. Su, A review of geometry-confined perovskite morphologies: From synthesis to efficient optoelectronic applications, *Nano Res.*, 2022, **15**, 7402–7431.
- S. Z. Wang, J. T. Wang, Y. H. Lou, Y. H. Zhou and Z. K. Wang, Environment-Friendly Perovskite Light-Emitting Diodes: Progress and Perspective, *Adv. Mater. Interfaces*, 2022, **9**, 2200772.
- S. Ju, Y. Zhu, H. Hu, Y. Liu, Z. Xu, J. Zheng, C. Mao, Y. Yu, K. Yang, L. Lin, T. Guo and F. Li, Dual-function perovskite light-emitting/sensing devices for optical interactive display, *Light: Sci. Appl.*, 2022, **11**, 331–339.
- A. Elattar, J. Kangsabanik, K. Nakao, K. Tsutsumi, H. Suzuki, T. Nishikawa, K. S. Thygesen and Y. Hayashia, Copper-incorporation for polytypism and bandgap engineering of MAPbBr<sub>3</sub> perovskite thin films with enhanced near-Infrared photocurrent-response, *Mater. Chem. Front.*, 2022, **6**, 2690–2702.
- Z. T. Li, H. W. Zhang, J. S. Li, K. Cao, Z. Chen, L. Xu, X. R. Ding, B. H. Yu, Y. Tang, J. Z. Ou, H. C. Kuo and H. L. Yip, Perovskite-Gallium Nitride Tandem Light-Emitting Diodes with Improved Luminance and Color Tunability, *Adv. Sci.*, 2022, **9**, 2201844.
- C. Otero-Martinez, J. Ye, J. Sung, I. Pastoriza-Santos, J. Perez-Juste, Z. Xia, A. Rao, R. L. Z. Hoyer and L. Polavarapu, Colloidal Metal-Halide Perovskite Nanoplatelets: Thickness-Controlled Synthesis, Properties, and Application in Light-Emitting Diodes, *Adv. Mater.*, 2022, **34**, 2107105.
- Y. Xu, M. Cao and S. Huang, Recent advances and perspective on the synthesis and photocatalytic application of metal halide perovskite nanocrystals, *Nano Res.*, 2021, **14**, 3773–3794.
- Z. K. Tan, R. S. Moghaddam, M. L. Lai, P. Docampo, R. Higler, F. Deschler, M. Price, A. Sadhanala, L. M. Pazos, D. Credgington, F. Hanusch, H. J. Snaith and R. H. Friend, Bright lightemitting diodes based on organometal halide perovskite, *Nat. Nanotechnol.*, 2014, **9**, 687–692.
- K. Lin, J. Xing, L. N. Quan, F. P. G. de Arquer, X. Gong, J. Lu, L. Xie, W. Zhao, D. Zhang, C. Yan, W. Li, X. Liu, Y. Lu, J. Kirman, E. H. Sargent, Q. Xiong and Z. Wei, Perovskite light-emitting diodes with external quantum efficiency exceeding 20 percent, *Nature*, 2018, **562**, 245–248.
- Y. Cao, N. Wang, H. Tian, J. Guo, Y. Wei, H. Chen, Y. Miao, W. Zou, K. Pan, Y. He, H. Cao, Y. Ke, M. Xu, Y. Wang, M. Yang, K. Du, Z. Fu, D. Kong, D. Dai, Y. Jin, G. Li, H. Li, Q. Peng, J. Wang and W. Huang, Perovskite light-emitting diodes based on spontaneously formed submicrometre-scale structures, *Nature*, 2018, **562**, 249–253.
- T. Chiba, Y. Hayashi, H. Ebe, K. Hoshi, J. Sato, S. Sato, Y. J. Pu, S. Ohisa and J. Kido, Anion-exchange red perovskite quantum dots with ammonium iodine salts for highly efficient light-emitting devices, *Nat. Photon.*, 2018, **12**, 681–687.
- Y. Dong, Y. K. Wang, F. Yuan, A. Johnston, Y. Liu, D. Ma, M. J. Choi, B. Chen, M. Chekini, S. W. Baek, L. K. Sagar, J. Fan, Y. Hou, M. Wu, S. Lee, B. Sun, S. Hoogland, R. Q. Bermudez, H. Ebe, P. Todorovic, F. Dinic, P. Li, H. T. Kung, M. I. Saidaminov, E. Kumacheva, E. Spiecker, L. S. Liao, O. Voznyy, Z. H. Lu and E. H. Sargent, Bipolar-shell resurfacing for blue LEDs based on strongly confined perovskite quantum dots, *Nat. Nanotechnol.*, 2020, **15**, 668–674.
- J. S. Kim, J. M. Heo, G. S. Park, S. J. Woo, C. Cho, H. J. Yun, D. H. Kim, J. Park, S. C. Lee, S. H. Park, E. Yoon, N. C. Greenham and T. W. Lee, Ultra-bright, efficient and stable perovskite light-emitting diodes, *Nature*, 2022, **611**, 688–694.
- M. Qin, P. F. Chan and X. Lu, A Systematic Review of Metal Halide Perovskite Crystallization and Film Formation Mechanism Unveiled by In Situ GIWAXS, *Adv. Mater.*, 2021, **33**, 2105290.
- S. Tan, T. Huang and Y. Yang, Defect passivation of perovskites in high efficiency solar cells, *J. Phys. Energy*, 2021, **3**, 042003.
- C. Yan, K. Lin, J. Lu and Z. Wei, Composition engineering to obtain efficient hybrid perovskite light-emitting diodes, *Front. Optoelectron.*, 2020, **13**, 282–290.
- P. Barua and I. Hwang, Bulk Perovskite Crystal Properties Determined by Heterogeneous Nucleation and Growth, *Materials*, 2023, **16**, 2110–2138.
- D. Zhang, Y. Fu, H. Zhan, C. Zhao, X. Gao, C. Qin and L. Wang, Suppressing thermal quenching via defect passivation for efficient quasi-2D perovskite light-emitting diodes, *Light: Sci. Appl.*, 2022, **11**, 69–78.
- J. K. Mishra, N. Yantara, A. Kanwat, T. Furuhashi, S. Ramesh, T. Salim, N. F. Jamaludin, B. Febriansyah, Z. E. Ooi, S. Mhaisalkar, T. C. Sum, K. Hippalgaonkar and N. Mathews, Defect Passivation Using a Phosphonic Acid Surface Modifier for Efficient RP Perovskite Blue-Light-Emitting Diodes, *ACS Appl. Mater. Interfaces*, 2022, **14**, 34238–34246.
- M. Li, Y. Zhao, J. Guo, X. Qin, Q. Zhang, C. Tian, P. Xu, Y. Li, W. Tian, X. Zheng, G. Xing, W. H. Zhang and Z. Wei, Phase Regulation and Defect Passivation Enabled by Phosphoryl Chloride Molecules for Efficient Quasi-2D Perovskite Light-Emitting Diodes, *Nano-Micro Lett.*, 2023, **15**, 119–129.
- K. Lin, C. Yan, R. P. Sabatini, W. Feng, J. Lu, K. Liu, D. Ma, Y. Shen, Y. Zhao, M. Li, C. Tian, L. Xie, E. H. Sargent and Z. Wei, Dual-Phase Regulation for High-Efficiency Perovskite Light-Emitting Diodes, *Adv. Funct. Mater.*, 2022, **32**, 2200350.
- R. Yang, Y. Q. Li, M. L. Guo, X. Y. Cai and J. X. Tang, Efficient pure-red perovskite light-emitting diodes using dual-Lewis-base molecules for interfacial modification, *J. Mater. Chem. C*, 2021, **9**, 9169–9177.
- J. N. Yang, Y. Song, J. S. Yao, K. H. Wang, J. J. Wang, B. S. Zhu, M. M. Yao, S. U. Rahman, Y. F. Lan, F. J. Fan and



- H. B. Yao, Potassium Bromide Surface Passivation on CsPbI<sub>3-x</sub>Br<sub>x</sub> Nanocrystals for Efficient and Stable Pure Red Perovskite Light-Emitting Diodes, *J. Am. Chem. Soc.*, 2020, **142**, 2956–2967.
- 24 S. Bonabi Naghadeh, B. Luo, G. Abdelmageed, Y. C. Pu, C. Zhang and J. Z. Zhang, Photophysical Properties and Improved Stability of Organic-Inorganic Perovskite by Surface Passivation, *J. Phys. Chem. C*, 2018, **122**, 15799–15818.
- 25 M. Lu, X. Zhang, X. Bai, H. Wu, X. Shen, Y. Zhang, W. Zhang, W. Zheng, H. Song and W. W. Yu, Spontaneous Silver Doping and Surface Passivation of CsPbI<sub>3</sub> Perovskite Active Layer Enable Light-Emitting Devices with an External Quantum Efficiency of 11.2, *ACS Energy Lett.*, 2018, **3**, 1571–1577.
- 26 X. Yang, X. Zhang, J. Deng, Z. Chu, Q. Jiang, J. Meng, P. Wang, L. Zhang, Z. Yin and J. You, Efficient green light-emitting diodes based on quasi-two-dimensional composition and phase engineered perovskite with surface passivation, *Nat. Commun.*, 2018, **9**, 570–577.
- 27 L. Na Quan, D. Ma, Y. Zhao, O. Voznyy, H. Yuan, E. Bladt, J. Pan, F. P. Garcia de Arquer, R. Sabatini, Z. Piontkowski, A. H. Emwas, P. Todorović, R. Quintero-Bermudez, G. Walters, J. Z. Fan, M. Liu, H. Tan, M. I. Saidaminov, L. Gao, Y. Li, D. H. Anjum, N. Wei, J. Tang, D. W. McCamant, M. B. J. Roelofs, S. Bals, J. Hofkens, O. M. Bakr, Z. H. Lu and E. H. Sargent, Edge stabilization in reduced-dimensional perovskites, *Nat. Commun.*, 2020, **11**, 170–178.
- 28 M. Li, Y. Zhao, X. Qin, Q. Ma, J. Lu, K. Lin, P. Xu, Y. Li, W. Feng, W. H. Zhang and Z. Wei, Conductive Phosphine Oxide Passivator Enables Efficient Perovskite Light-Emitting Diodes, *Nano Lett.*, 2022, **22**, 2490–2496.
- 29 S. Wang, Z. Zhang, Z. Tang, C. Su, W. Huang, Y. Li and G. Xing, Polymer strategies for high-efficiency and stable perovskite solar cells, *Nano Energy*, 2021, **82**, 105712.
- 30 W. Feng, Y. Zhao, K. Lin, J. Lu, Y. Liang, K. Liu, L. Xie, C. Tian, T. Lyu and Z. Wei, Polymer-Assisted Crystal Growth Regulation and Defect Passivation for Efficient Perovskite Light-Emitting Diodes, *Adv. Funct. Mater.*, 2022, **32**, 2203371.
- 31 D. Ma, K. Lin, Y. Dong, H. Choubisa, A. H. Proppe, D. Wu, Y. K. Wang, B. Chen, P. Li, J. Z. Fan, F. Yuan, A. Johnston, Y. Liu, Y. Kang, Z. H. Lu, Z. Wei and E. H. Sargent, Distribution control enables efficient reduced-dimensional perovskite LEDs, *Nature*, 2021, **599**, 594–598.
- 32 W. Bai, T. Xuan, H. Zhao, H. Dong, X. Cheng, L. Wang and R. J. Xie, Perovskite light-emitting diodes with an external quantum efficiency exceeding 30%, *Adv. Mater.*, 2023, DOI: [10.1002/adma.202302283](https://doi.org/10.1002/adma.202302283).
- 33 L. Kong, X. Zhang, C. Zhang, L. Wang, S. Wang, F. Cao, D. Zhao, A. L. Rogach and X. Yang, Stability of Perovskite Light-Emitting Diodes: Existing Issues and Mitigation Strategies Related to Both Material and Device Aspects, *Adv. Mater.*, 2022, **34**, 2205217.
- 34 V. J. Y. Lim, A. M. Ulatowski, C. Kamaraki, M. T. Klug, L. Miranda Perez, M. B. Johnston and L. M. Herz, Air-Degradation Mechanisms in Mixed Lead-Tin Halide Perovskites for Solar Cells, *Adv. Energy Mater.*, 2022, 2200847.
- 35 Y. Nakamura, N. Shibayama, K. Fujiwara, T. Koganezawa and T. Miyasaka, Degradation Mechanism of Halide Perovskite Crystals under Concurrent Light and Humidity Exposure, *ACS Mater. Lett.*, 2022, **4**, 2409–2414.
- 36 P. Du, L. Gao and J. Tang, Focus on performance of perovskite light-emitting diodes, *Front. Optoelectron.*, 2020, **13**, 235–245.
- 37 J. T. Wang, S. Z. Wang, Y. H. Zhou, Y. H. Lou and Z. K. Wang, Flexible perovskite light-emitting diodes: Progress, challenges and perspective, *Sci. China Mater.*, 2022, **66**, 1–21.
- 38 G. Li, K. Chen, Y. Cui, Y. Zhang, Y. Tian, B. Tian, Y. Hao, Y. Wu and H. Zhang, Stability of Perovskite Light Sources: Status and Challenges, *Adv. Opt. Mater.*, 2020, **8**, 1902012.
- 39 N. Li, Y. Jia, Y. Guo and N. Zhao, Ion Migration in Perovskite Light-Emitting Diodes: Mechanism, Characterizations, and Material and Device Engineering, *Adv. Mater.*, 2022, **34**, 2108102.
- 40 C. J. Tong, X. Cai, A. Y. Zhu, L. M. Liu and O. V. Prezhdo, How Hole Injection Accelerates Both Ion Migration and Non-radiative Recombination in Metal Halide Perovskites, *J. Am. Chem. Soc.*, 2022, **144**, 6604–6612.
- 41 Q. Dong, L. Lei, J. Mendes and F. So, Operational stability of perovskite light emitting diodes, *J. Phys.: Mater.*, 2020, **3**, 012002.
- 42 S. Z. Wang, J. T. Wang, Y. H. Lou, Y. H. Zhou and Z. K. Wang, Environment-Friendly Perovskite Light-Emitting Diodes: Progress and Perspective, *Adv. Mater. Interfaces*, 2022, **9**, 2200772.
- 43 J. Lu, X. Guan, Y. Li, K. Lin, W. Feng, Y. Zhao, C. Yan, M. Li, Y. Shen, X. Qin and Z. Wei, Dendritic CsSnI<sub>3</sub> for Efficient and Flexible Near-Infrared Perovskite Light-Emitting Diodes, *Adv. Mater.*, 2021, **33**, 2104414.
- 44 L. Kong, X. Zhang, Y. Li, H. Wang, Y. Jiang, S. Wang, M. You, C. Zhang, T. Zhang, S. V. Kershaw, W. Zheng, Y. Yang, Q. Lin, M. Yuan, A. L. Rogach and X. Yang, Smoothing the energy transfer pathway in quasi-2D perovskite films using methanesulfonate leads to highly efficient light-emitting devices, *Nat. Commun.*, 2021, **12**, 1246–1253.
- 45 C. Sun, Y. Jiang, M. Cui, L. Qiao, J. Wei, Y. Huang, L. Zhang, T. He, S. Li, H. Y. Hsu, C. Qin, R. Long and M. Yuan, High-performance large-area quasi-2D perovskite light-emitting diodes, *Nat. Commun.*, 2021, **12**, 2207–2217.
- 46 L. Gu, K. Wen, Q. Peng, W. Huang and J. Wang, Surface-Plasmon-Enhanced Perovskite Light-Emitting Diodes, *Small*, 2020, **16**, 2001861.
- 47 Q. Zhang, M. M. Tavakoli, L. Gu, D. Zhang, L. Tang, Y. Gao, J. Guo, Y. Lin, S. F. Leung, S. Poddar, Y. Fu and Z. Fan, Efficient metal halide perovskite light-emitting diodes with significantly improved light extraction on nanophotonic substrates, *Nat. Commun.*, 2019, **10**, 727–735.
- 48 Y. Miao, L. Cheng, W. Zou, L. Gu, J. Zhang, Q. Guo, Q. Peng, M. Xu, Y. He, S. Zhang, Y. Cao, R. Li, N. Wang, W. Huang and J. Wang, Microcavity top-emission perovskite light-emitting diodes, *Light: Sci. Appl.*, 2020, **9**, 89–94.